Synthesis and CO_2 Capture Properties of Nanocrystalline Lithium Zirconate

Esther Ochoa-Fernández,[†] Magnus Rønning,[†] Tor Grande,[‡] and De Chen*,[†]

Departments of Chemical Engineering and Materials Science and Engineering, Norwegian University of Science and Technology, Sem Sælands vei 4, NO-7491 Trondheim, Norway

Received June 30, 2006. Revised Manuscript Received August 30, 2006

Nanocrystalline tetragonal Li_2ZrO_3 was prepared by a novel soft-chemistry route, resulting in powders with good properties for CO_2 capture at high temperatures. The CO_2 capture and regeneration properties of the material were investigated by a tapered element oscillating microbalance (TEOM) in a wide range of temperatures and partial pressures of CO_2. The nanocrystalline tetragonal Li_2ZrO_3 has superior CO_2 capture and regeneration properties compared to monoclinic Li_2ZrO_3 prepared by solid-state synthesis. Moreover, the regeneration could be performed at a lower temperature, and a high stability of the CO_2 capture/regeneration capacity was observed. The nanocrystalline tetragonal Li_2ZrO_3 opens new opportunities for the application of solid acceptors in CO_2 capture in both post- and precombustion processes in power generation.

1 Introduction

The global consumption of energy and the associated emissions of carbon dioxide have continuously shown a rising trend during the last decades. According to the Intergovernmental Panel on Climate Change (IPCC),[1] fossil fuels are the dominant form of energy utilized in the world (86%) and account for about 75% of the current anthropogenic CO_2 emissions. The CO_2 emissions from various sectors have been estimated by the International Energy Agency (IEA),[2] and power generation is the single largest source of emission, followed by other energy industries such as oil refineries, manufacture of solid fuels, coal mining, and oil and gas extraction.

There exist different initiatives to mitigate the increase of the carbon dioxide emissions.[3] Reductions in the fossil fuel consumption can be achieved by improving the efficiency of energy conversion, for example, by the use of improved turbines. Another way to minimize the emissions is to switch to less-carbon-intensive fossil fuels as natural gas and/or increase the use of low- and near-zero-carbon energies, such as renewable energy or nuclear power. These measures can reduce the CO_2 generation; however, in order to reach the specific atmospheric CO_2 levels set in different international agreements, the capture of CO_2 and its storage may play a very important role.

The approach consists of capturing CO_2 generated by combustion or CO_2 released from different industrial processes and storing it away from the atmosphere for a long time. The main application studied so far for CO_2 capture is its use in power generation. For this purpose, it is possible to have different systems:[4]

- Postcombustion capture: capture of CO_2 from the flue gases produced after combustion of fossil fuels.
- Oxy-fuel combustion capture: oxygen is used as combustion agent, producing a flue gas that consists mainly of steam and CO_2.
- Precombustion capture: the CO_2 is removed before the combustion of hydrogen, where the hydrogen is produced, for example, by reforming of hydrocarbons.

There exist different technologies for CO_2 separation. The most studied are separation with sorbents (liquid absorbent or solid acceptors) and separation with selective membranes.[5] In the present work, selective CO_2 capture at high temperatures by solid acceptors is addressed.

The use of regenerable solid acceptors at high temperatures might have various applications in both pre- and postcombustion systems. The flue gases produced after the combustion of fossil fuels in a turbine are usually in the temperature range from 700 to 900 K. Thus, they need to be cooled to the temperature levels required for the absorption process in case a wet-absorption method is chosen for separation. However, the removal of the carbon dioxide at high temperatures by the use of solid acceptors has the potential to reduce efficiency penalties compared to the wet-absorption methods.[3] In this case, the combustion flue gas is put in direct contact with the CO_2 acceptor, and a gas−solid reaction of the CO_2 with the acceptor takes place. Accordingly, the CO_2

* Corresponding author. Fax: 47 73 59 40 80. Telephone: 47 73 59 31 49. E-mail: chen@chemeng.ntnu.no.

[†] Department of Chemical Engineering, Norwegian University of Science and Technology.

[‡] Department of Materials Science and Engineering, Norwegian University of Science and Technology.

(1) *IPCC Third Assessment Report−Climate Change 2001*; International Panel on Climate Change: Geneva, Switzerland, 2001.

(2) *Prospects for Carbon Dioxide Capture and Storage*; International Energy Agency: Paris, 2004.

(3) *IPCC Special Report on Carbon Dioxide Capture and Storage*; Intergovernmental Panel on Climate Change: Geneva, Switzerland, 2005.

(4) Ertesvåg, I. S.; Kvamsdal, H. M.; Bolland, O. *Energy* **2005**, *30*, 5.

(5) Bredesen, R.; Jordal, K.; Bolland, O. *Chem. Eng. Process.* **2004**, *43*, 1129.

10.1021/cm061515d CCC: $33.50
Published on Web 11/09/2006

is selectively removed from the flue gas stream until saturation of the solid acceptor. At this time, the acceptor can easily be separated from the gas and regenerated.

CO_2 sorption-enhanced steam methane reforming (SESMR) is also an important application of CO_2 acceptors in hydrogen production and/or precombustion processes.[6−15] SESMR is an alternative to conventional steam reforming, in which a CO_2 acceptor is installed together with the catalyst in the reactor. In this way, the reaction equilibrium is shifted toward H_2 production. Much higher H_2 yields are obtained at lower temperatures (723−873 K) with a simpler process layout. There is no need for water−gas shift reactors or absorption columns and there are less-demanding requirements for the reactor materials because of low operating temperatures. The main challenge, however, is to develop an acceptor with fast kinetics, easy regeneration, high stability, and high carbon-dioxide-capture capacity at the working temperatures.

There has been extensive research on the uptake of CO_2 on acceptors at ambient temperature and atmospheric pressure. However, there are few relevant investigations about the capture of CO_2 at high temperatures and pressures. Different materials have been proposed in the literature.[16−21] Yong et al.[22] have reported that carbon-based sorbents have adequate capacity for CO_2 at relatively low temperatures (298−523 K). The capture capacity of these materials is reduced when the capture temperature is further increased (>523 K). Different zeolites have also been reported to work in the same range.[20] Hydrotalcite-like compounds are able to accept CO_2 at a wider range of temperatures, up to 673 K. However, these compounds lose more than half of their capacity after several cycles. The same problem has been found in the use of calcium-based acceptors. The regeneration of Ca-based acceptors is highly energy demanding. The use of high temperatures for the regeneration leads to sintering and subsequent pore blockage and losses in the porosity. In addition, CaO can react with steam under the reaction conditions, leading to the formation of $Ca(OH)_2$ and thus lowering the methane conversion and hydrogen yield.[23] The development of an acceptor with relatively low temperatures for regeneration and with good multicycle properties is highly desirable. Recently, it has been reported that Li-containing materials are promising candidates with high CO_2 capture capacity and high stability.[24−39]

Nakagawa et al. have reported that lithium zirconate and lithium silicate can theoretically hold CO_2 in amounts up to, respectively, 28 and 36 acceptor weight percent at high temperatures according to the following equations[33]

$$Li_2ZrO_3 + CO_2 \leftrightarrow Li_2CO_3 + ZrO_2 \quad (1)$$

$$Li_4SiO_4 + CO_2 \leftrightarrow Li_2CO_3 + Li_2SiO_3 \quad (2)$$

The high capture capacity and stability at 723−873 K for these materials make them very promising for application in both pre- and postcombustion systems. However, kinetic limitations during the CO_2 capture are still the main obstacle.

The synthesis of lithium-containing ceramic powder has been extensively studied, and in particular lithium zirconate, as it is one of the candidates of the tritium breeding for nuclear fusion reactors. Various solid-state processes have been employed to fabricate the lithium zirconate powders. Solid-state reactions between ZrO_2 and lithium peroxide (or carbonate) are the best known processes.[30,33,40] In these processes, two types of powders are mechanically mixed and treated at high temperatures. Solid-state reactions normally require high temperatures and long reaction times. For example, Ida et al.[31] prepared pure Li_2ZrO_3 powder with particle diameters larger than 1 μm by solid-state reaction of Li_2CO_3 and ZrO_2. The final particle size of the powder prepared by solid-state methods is normally large, partially due to sintering during the high-temperature treatment. The particle size is also very much controlled by the particle size of the starting ZrO_2. Xiong et al. studied the CO_2 capture on Li_2ZrO_3 synthesized by ZrO_2 of two different sizes (1 and 45 μm).[24] For 45 μm ZrO_2-derived Li_2ZrO_3, particles were isolated from each other and the particles had an average size around 30 μm. For 1 μm ZrO_2-derived Li_2ZrO_3, however, the average particle size was 10 μm.

There have been several efforts to reduce the starting powder size for solid-state processes. One example is the

(6) Hufton, F. R.; Mayorga, S.; Sircar, S. *AIChE J.* **1999**, *45*, 248.
(7) Ding, Y.; Alpay, E. *Chem. Eng. Sci.* **2000**, *55*, 3929.
(8) Waldron, W. E.; Hufton, J. R.; Sircar, S. *AIChE J.* **2001**, *47*, 1477.
(9) Lopez-Ortiz, A.; Harrison, D. P. *Ind. Eng. Chem. Res.* **2001**, *40*, 5102.
(10) Xiu, G.-h.; Li, P.; Rodriges, A. E. *Chem. Eng. Sci.* **2002**, *57*, 3893.
(11) Xiu, G.-h.; Li, P.; Rodrigues, A. E. *Chem. Eng. Sci.* **2003**, *58*, 3425.
(12) Abanades, J. C.; Anthony, E. J.; Wang, J.; Oakey, J. E. *Environ. Sci. Technol.* **2005**, *39*, 2861.
(13) Kato, M.; Maezawa, Y.; Takeda, S.; Hagiwara, Y.; Kogo, R. *J. Ceram. Soc. Jpn.* **2005**, *113*, 252.
(14) Wang, Y.-N.; Rodrigues, A. E. *Fuel* **2005**, *84*, 1778.
(15) Ochoa-Fernández, E.; Rusten, H. K.; Jakobsen, H. A.; Rønning, M.; Homen, A.; Chen, D. *Catal. Today* **2005**, *106*, 41.
(16) Yong, Z.; Mata, V.; Rodrigues, A. E. *Ind. Eng. Chem. Res.* **2001**, *40*, 204.
(17) Yong, Z.; Rodrigues, A. E. *Energy Convers. Manage.* **2002**, *43*, 1865.
(18) Ding, Y.; Alpay, E. *Chem. Eng. Sci.* **2000**, *55*, 3461.
(19) Siriwardane, R.; Shen, M.; Poston, J.; Shamsi, A. U.S. Department of Energy, National Energy Technology Laboratory: Pittsburgh, PA, 2002.
(20) Yong, Z.; Mata, V.; Rodrigues, A. E. *Sep. Purif. Technol.* **2002**, *26*, 195.
(21) Pfeiffer, H.; Bosch, P. *Chem. Mater.* **2005**, *17*, 1704.
(22) Yong, Z.; Mata, V. G.; Rodrigues, A. E. *Adsorption* **2001**, *7*, 41.
(23) Hildengrand, N.; Readman, L.; Dahl, I. M.; Blom, R. *Appl. Catal., A* **2006**, *303*, 131.
(24) Xiong, R.; Ida, J.; Lin, Y. S. *Chem. Eng. Sci.* **2003**, *58*, 4377.
(25) Ida, J. I.; Xiong, R.; Lin, Y. S. *Sep. Purif. Technol.* **2003**, 1.
(26) Kato, M.; Yoshikawa, S.; Nakagawa, K. *J. Mater. Sci. Lett.* **2002**, *21*, 485.
(27) Nair, B. N.; Yamaguchi, T.; Kawamura, H.; Nakao, S.-I. *J. Am. Ceram. Soc.* **2004**, *87*, 68.
(28) Essaki, K.; Nakagawa, K.; Kato, M.; Uemoto, H. *J. Chem. Eng. Jpn.* **2004**, *37*, 772.
(29) Ohashi, T.; Nakagawa, K. *Mat. Res. Soc. Symp. Proc.* **1999**, *547*, 249.
(30) Kato, M.; Nakagawa, K. *J. Ceram. Soc. Jpn.* **2001**, *109*, 911.
(31) Ida, J.; Lin, Y. S. *Environ. Sci. Technol.* **2003**, *37*, 1999.
(32) Yoshikawa, S.; Kato, M.; Essaki, K.; Nakagawa, K.; Uemoto, H. *Proc. Can. Cancer Conf.* **2001**, *18*, 563.
(33) Nakagawa, K.; Ohashi, T. *J. Electrochem. Soc.* **1998**, *145*, 1344.
(34) Lopez-Ortiz, A.; Rivera, N. G. P.; Rojas, A. R.; Gutierrez, D. L. *Sep. Sci. Tech.* **2004**, *39*, 3559.
(35) Fauth, D. J.; Hoffman, J. S.; Pennline, H. W. *J. Environ. Technol. Manage.* **2004**, *4*, 68.
(36) Kimura, S.; Adachi, M.; Noda, R.; Horio, M. *Chem. Eng. Sci.* **2005**, *60*, 4061.
(37) Fauth, D. J.; Frommell, E. A.; Hoffman, J. S.; Reasbeck, R. P.; Pennline, H. W. *Fuel Process. Technol.* **2005**, *86*, 1503.
(38) Ochoa-Fernández, E.; Grande, T.; Rønning, M.; Chen, D. *Chem. Mater.* **2006**, *18*, 1383.
(39) Yi, K. B.; Eriksen, D. Ø. *Sep. Sci. Technol.* **2006**, *41*, 283.
(40) Alvani, C.; Bruzzi, L.; Casadio, S.; Rondinella, V.; Tucci, A.; Toscano, E. H. *J. Eur. Chem. Soc.* **1989**, *5*, 295.

use of a sol−gel technique to prepare fine powders of ZrO_2.[27] However, this powder is subsequently reacted in the solid state with Li_2ZrO_3 at high temperatures with following sintering problems.

A precipitation combustion process has also been reported to synthesize Li_2ZrO_3 powder as breeding material for fusion reactors.[41] Li_2ZrO_3 can easily be obtained by this method using a mixture of urea and citric acid in stoichiometric composition. The primary particle size of these powders was smaller than 20 nm. However, the powder contains some impurities and requires high calcination temperatures. There are other wet-chemistry routes reported for the preparation of Li_2ZrO_3 as a breeding material. Alvani et al. developed two wet routes starting from metal alkoxides, where temperatures higher than 1073 K were required for the preparation of Li_2ZrO_3.[40] Montanaro et al. proposed a gelling method using lithium acetate and zirconium propylate as precursors.[42] However, this method yielded particle sizes larger than 40 μm.

Recently, Nair et al.[27] have done a systematic study on the properties of Li_2ZrO_3 with different crystal structures. They have compared the properties of powders prepared by solid-state reactions of mixed powders, sol−gel prepared powders, and commercial grade powder. Their results indicated that tetragonal Li_2ZrO_3 powders show a larger rate of sorption than their monoclinic counterparts. They also concluded that small particle size is critical to enhancing the CO_2 capture. The same conclusion was reached by Yi et al. after they prepared tetragonal Li_2ZrO_3 by a low-temperature liquid-state synthesis.[39]

We have recently reported a novel soft-chemistry preparation route for the synthesis of nanocrystalline Li_2ZrO_3.[15,38,43] This preparation method represents several advantages.[38] In short, the method yields pure nanocrystals of Li_2ZrO_3 with pure tetragonal phase using relatively low calcination temperatures. As a result, the properties of the powders such as the capture rate of CO_2 and regeneration temperature have been significantly improved.

The present work deals with a detailed characterization of the materials and kinetic study of CO_2 capture and regeneration at high temperatures, aiming at a better understanding of the relationship between the crystalline structure of the materials and their properties as a CO_2 acceptor. Thus, a detailed study of the structure and morphology of the acceptor has been carried out using different techniques, such as (in situ) XRD, SEM, and BET measurements. The CO_2 capture/regeneration properties of the material have been monitored over a wide temperature range and partial pressures of CO_2 using a tapered element oscillating microbalance.

2 Experimental Section

2.1. Preparation of Lithium Zirconate. Zirconyl nitrate ($ZrO(NO_3)_2 \cdot xH_2O$, Fluka) and lithium acetate ($CH_3COOLi \cdot 2H_2O$, Fluka) were used as precursors as described elsewhere.[38,43] Appropriate amounts of each precursor were dissolved in deionized water. After standardization of the solutions by thermogravimetric analysis, the precursors were mixed for several hours in appropriate amounts to form a complex solution. The solution was spray dried (Büchi, Mini Spray-Drier B-191) with an input temperature of 423 K and a pump rate of 2 mL/min. The resulting solid products were further decomposed/oxidized in a certain temperature range, forming powders with a homogeneous atomic mixture of Li and Zr. The powders were calcined at three different temperatures in air, leading to decomposition of the organic compounds by a smouldering reaction. As an alternative drying route to the spray drying, a fraction of the precursor solution was solidified by heating to 373 K in an oil bath under continuous stirring. The sample prepared by spray drying is referred to as Li_2ZrO_3-SD, whereas the second sample is referred to as Li_2ZrO_3-D.

2.2. Lithium Zirconate Characterization. *2.2.1. X-ray Diffraction.* X-ray diffraction patterns were recorded at room temperature on a Siemens D5005 X-ray diffractometer using Cu $K\alpha$ radiation ($\lambda = 1.54$ Å). The scans were recorded in the 2θ range between 20 and 85° using a step size of 0.03°.

The average crystallite thickness was calculated from the Scherrer equation[44] using the (020) lithium zirconate peak located at $2\theta = 42.3°$. Lanthanum hexaboride, LaB_6, was used as reference material to determine the instrumental line broadening.

In addition, the powders were also studied by in situ high-temperature X-ray diffraction (in situ HTXRD) using a Siemens D5005 diffractometer equipped with a position sensitive detector (PSD-50M, MBRAUN). The powders were dispersed in ethanol and applied on a platinum strip located in a high-temperature camera (HTK16, Anton Paar GmbH). The data were collected with a step size of 0.0364° and a step time of 0.5 s. The capture reaction was carried out at 848 K under a CO_2-containing atmosphere. The regeneration was carried out at 943 K under a flow of nitrogen. Scans were recoded every 10 min.

2.2.2. N_2 Physisorption. Nitrogen adsorption−desorption isotherms were measured with a Micromeritics TriStar 3000 instrument, and the data were collected at liquid nitrogen temperature, 77 K. The samples were outgassed at 573 K overnight prior to measurement.

The surface area was calculated from the Brunauer−Emmett−Teller (BET) equation,[45] whereas the total pore volume and the average pore size were calculated by applying the Barrett−Joyner−Halenda (BJH) method.[46]

2.2.3. Hg Porosimetry. Pore size measurements were also performed using a Carlo Erba Porosimeter 2000 by mercury intrusion. Each sample was evacuated and dried at 423 K prior to analysis. A cylindrical pore model was assumed.

2.2.4. Field Emission Scanning Electron Microscopy. The morphology of the Li_2ZrO_3 powders was examined in a Hitachi S-4300se field emission scanning electron microscope (SEM) equipped with a field emission gun with Schottky emitter. The acceleration voltage was set to 5 kV, and the secondary electron detector was used. The samples were prepared by dropping some lithium zirconate fine powder onto a wet carbon tape. The samples were also coated with a fine layer of carbon to enhance the conductivity.

(41) Park, J. Y.; Jung, C. J.; Oh, S.-J.; Park, H. K.; Kim, Y. S. *Ceram. Trans.* **1997**, *85*, 55.
(42) Montanaro, L.; Lecompte, J. P. *J. Mater. Sci.* **1992**, *27*, 3763.
(43) Chen, D.; Ochoa-Fernández, E.; Rønning, M.; Grande, T. Patent application O. nr. 110520.
(44) Scherrer, P. *Göttingen Nachrichten* **1918**, *2*, 98.
(45) Brunauer, S.; Emmett, P. H.; Teller, E. *J. Am. Chem. Soc.* **1938**, *60*, 309.
(46) Barret, E. P.; Joyner, L. G.; Halenda, P. P. *J. Am. Chem. Soc.* **1951**, *73*, 373.

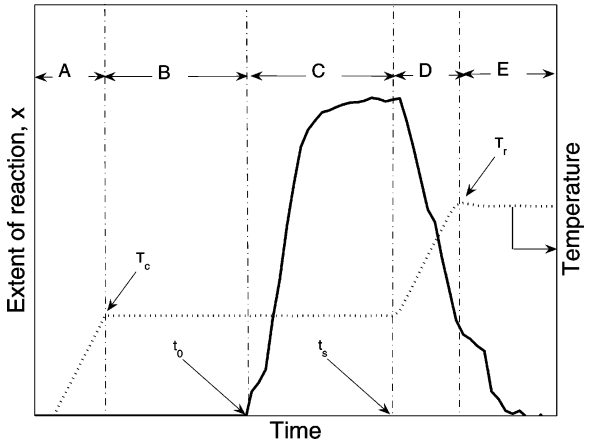

Figure 1. Scheme of the general procedure followed for the testing of the CO_2 capture properties of the prepared acceptors.

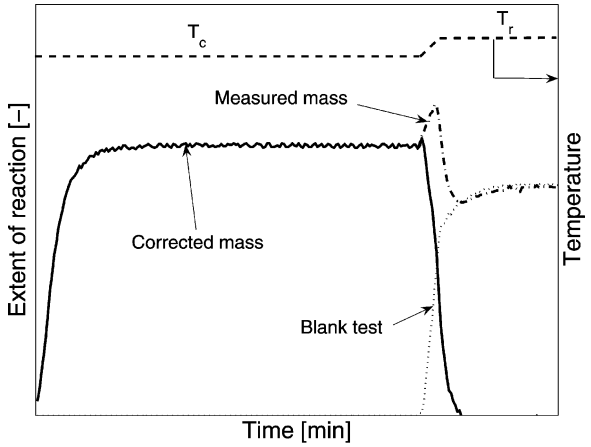

Figure 2. Scheme of the general procedure followed for the correction of no isothermal density change.

2.3. Thermodynamic Study. FactSage[47] has been used to study the thermodynamics of the system.

2.4. Kinetic Study of CO_2 Capture and Regeneration. CO_2 capture properties were evaluated using a tapered element oscillating microbalance (TEOM). The measurement of the mass change in the sample bed is based on changes in the natural frequency of an oscillating quartz element containing the sample. The main advantage of the TEOM is that all the gases are forced to flow through the catalyst bed, avoiding the bypass problem associated with a conventional microbalance. Thus, the sample bed can be treated as a fixed-bed reactor, and operation under differential conditions can be easily realized.[48] Moreover, operation without mass or heat diffusion limitations is possible, resulting in a better quantification of the CO_2 in the kinetic study. In addition, high mass resolution and short response time make the TEOM particularly suitable for performing the uptake measurements and kinetic study.[49] Details about the experimental set up have been reported elsewhere.[48] The tapered element was loaded with 20−30 mg of Li_2ZrO_3 together with quartz particles. An illustration of the experimental procedure is given in Figure 1. The extent of the reaction is plotted versus the capture time. The extent of the reaction, x, is defined as $x = \Delta w/\Delta w_{max}$, where Δw and Δw_{max} are the measured and the maximum experimental uptake of CO_2, respectively.

- Period A: The sample was heated to the capture temperature (T_c) under 100 mL/min of Ar with a heating rate of 10 K/min. The maximum operating temperature for the TEOM reactor is 953 K.
- Period B: The sample was kept at T_c under an Ar atmosphere for stabilization of the weight.
- Period C: The Ar atmosphere was switched to the reaction mixture at a time t_0. The different partial pressures of CO_2 in the reaction mixture were obtained by adjusting the flow rates of Ar and CO_2 at a constant flow rate of 100 mL/min. During period C, the CO_2 capture takes place according to eq 1. This period is finished when no further increase in the extent of the reaction is observed. At this time, t_s, the acceptor is saturated.
- Period D: The reaction atmosphere was changed from the reaction mixture to pure Ar at a constant flow rate of 100 mL/min. To proceed with the regeneration of the acceptor, we also increased the temperature of the reactor from T_c to T_r (regeneration temperature) with a heating rate of 10 K/min.
- Period E: The reaction temperature was kept at T_r until the sample was completely regenerated.
- After period E, a new cycle was performed.

The experiments were carried out at different CO_2 partial pressures and capture/regeneration temperatures.

Because of the operating principle of TEOM, the mass of the gas occupied in the void volume in the tapered element affects the vibrational frequency of the balance. A mass change is detected when switching from one gas to another at isothermal conditions.[50] This mass change is proportional to the density difference between the two gases according to eq 3

$$\Delta m = \frac{V_e P(M_2 - M_1)}{RT} \tag{3}$$

where M_2 is the average molecular weight of the feed mixture (CO_2/Ar mixture in this study), M_1 is the molecular weight of the inert gas (Ar), Δm is the measured mass change, V_e is the void volume in the tapered element, T is the temperature, P is the pressure, and R is the ideal gas constant. The void volume of the tapered element is approximately 1 mL, and the molecular weight difference between the two switching gases (CO_2 and Ar) is very small. Thus, the mass change related to the density change in this system was always measured in the range 1×10^{-5} g to 1×10^{-6} g at the operation conditions. These values are negligible compared to the total mass change during the capture reaction, and consequently, no corrections related to the density change were necessary during the isothermal operation.

However, a temperature-programmed process was carried out during the regeneration step. In this case, the recorded apparent change on the mass is due to the release of CO_2 and changes in the reactor material properties, which result in changes on the vibrational frequency at different temperatures. A blank experiment is necessary in order to obtain the real mass change. An example is presented in Figure 2. The dash-dotted line represents the extent of the reaction directly measured during a typical capture experiment. The starting and final points are at different temperatures and cannot be directly compared. The dotted line represents a blank experiment, where the same capture/regeneration cycle is repeated under inert atmosphere, with no CO_2 addition in this case. This cycle gives a direct indication of the mass change due to the temperature switch. Subtracting the blank experiment from the direct measurement gives the mass change due to the CO_2 release (solid

(47) *FactSage 5, the Integrated Thermodynamic Databank System*; www.factsage.com.
(48) Chen, D.; Grøvold, A.; Rebo, H. P.; Moljord, K.; Holmen, A. *Appl. Catal.* **1996**, *137*, L1.
(49) Chen, D.; Rebo, H. P.; Moljord, K.; Homen, A. *Chem. Eng. Sci.* **1996**, *51*, 2687.
(50) Chen, D.; Moljord, K.; Rebo, H. P.; Holmen, A. *Ind. Eng. Chem. Res.* **1999**, *38*, 4242.

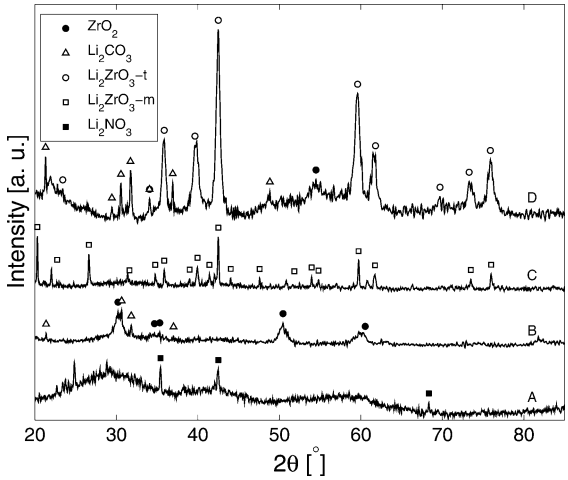

Figure 3. X-ray diffraction patterns of lithium zirconate prepared by spray drying and calcined at (A) uncalcined, (B) 670, (C) 1073, and (D) 873 K (○ = Li_2ZrO_3-*t*, □ = Li_2ZrO_3-*m*, Δ = Li_2CO_3, ● = ZrO_2, ■ = $LiNO_3$).

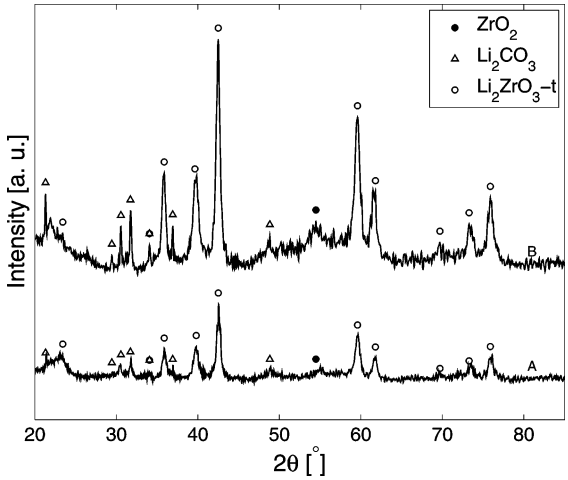

Figure 4. X-ray diffraction patterns of (A) Li_2ZrO_3-D and (B) Li_2ZrO_3-SD, both calcined at 873 K (Δ = Li_2CO_3, ● = ZrO_2, ○ = Li_2ZrO_3-*t*).

line in Figure 2). All the regeneration curves showed in this study have been corrected according to this procedure.

3. Results and Discussion

3.1. Lithium Zirconate Characterization. *3.1.1. X-ray Diffraction.* X-ray diffraction patterns of the prepared sample after spray drying and after subsequent calcination at different temperatures are given in Figure 3. A white powder with good flow ability is obtained after both spray drying and conventional drying. As shown in Figure 3A, the X-ray diffraction profile of the uncalcined powder after spray drying indicates the formation of an amorphous solid, where only lithium nitrate is identified as a crystalline phase. In the case of the powders dried by heating in a hot plate, indications of other mixed nitrates were also found. However, no traces of lithium zirconate were identified after drying. Further heat treatment is necessary in order to decompose the nitrates and the organometallic salts originating from the starting precursors.

The powders were calcined at three different temperatures: 673, 873, and 1073 K, respectively. Calcination at 673 K did not yield a pure Li_2ZrO_3, as shown in Figure 3B. A mixture of ZrO_2 and Li_2CO_3 was found. The formation of nanocrystals of Li_2ZrO_3 with pure tetragonal phase was observed when the calcination temperature was 873 K. However, small traces of Li_2CO_3 and ZrO_2 still seem to be present. The crystallite size of the Li_2ZrO_3 prepared after calcination at 873 K was calculated using the Scherrer equation[44] and was 13 and 14 nm for the spray dried sample (Li_2ZrO_3-SD) and hot-plate-dried sample (Li_2ZrO_3-D), respectively. Figure 4 shows the X-ray diffractograms of Li_2ZrO_3-SD and Li_2ZrO_3-D when both were calcined at 873 K. No structural differences can be observed from the diffraction data. The same trend is observed for other calcination temperatures. A further increase in the calcination temperature to 1073 K led to the formation of a mixture of Li_2ZrO_3 polymorphs. Monoclinic Li_2ZrO_3 was found as the predominant crystalline phase in this case. The crystallite size was calculated to be 42 and 33 nm for Li_2ZrO_3-SD and Li_2ZrO_3-D, respectively.

A phase transformation is observed between 873 and 1073 K in Figure 3 by comparison of the diffractograms C and D. This is in good agreement with the observation by Wyers et al., in which tetragonal Li_2ZrO_3 recrystallizes to a monoclinic structure at temperatures above 975 K.[51] Apparently, the phase transition from tetragonal to monoclinic Li_2ZrO_3 proceeds irreversibly.

Nair et al.[27] have synthesized Li_2ZrO_3 with different crystalline structures and crystal sizes by different routes and studied their ability for capturing CO_2 at high temperatures. It was concluded that the crystalline structure of the oxide is detrimental to the carbonation reaction. Li_2ZrO_3 materials with tetragonal structure captured CO_2 faster than their monoclinic counterparts. However, it was difficult to separate the relative effects of particle size and crystalline structure, because the formation of the monoclinic phase involves a stronger heat treatment, resulting in crystal growth. Nevertheless, tetragonal phase and smaller crystal size enhanced the capture rates. Consequently, calcination of powders at 873 K is selected in the present work because it results in nanocrystals of tetragonal Li_2ZrO_3. As shown in Figure 3, a further increase in the calcination temperature resulted in crystal growth and phase transformation. Most of the previous efforts carried out on the development of Li_2ZrO_3 as a CO_2 acceptor have been done on pure/modified Li_2ZrO_3 prepared by solid-state reaction. The solid-state reaction process requires treatment at high temperatures (>1123 K) for long times. Under these conditions, monoclinic Li_2ZrO_3 is formed and sintering/grain growth of the material is favored. Thus, the main advantage of the soft-chemistry method compared to solid-state synthesis is that it yields nanocrystals of tetragonal Li_2ZrO_3. The maximum temperature involved during the synthesis process is the calcination temperature at 873 K.

3.1.2. SEM. Examples of SEM images of Li_2ZrO_3-SD and Li_2ZrO_3-D are presented in Figures 5 and 6, respectively. The results indicate that, in the case of Li_2ZrO_3-SD, the individual Li_2ZrO_3 crystallites agglomerate to form larger particles with a relatively uniform size between 1 and 5 μm. All particles display a characteristic geometry; large spheres

(51) Wyers, G. P.; Cordfunke, E. H. P. *J. Nucl. Mater.* **1989**, *168*, 24.

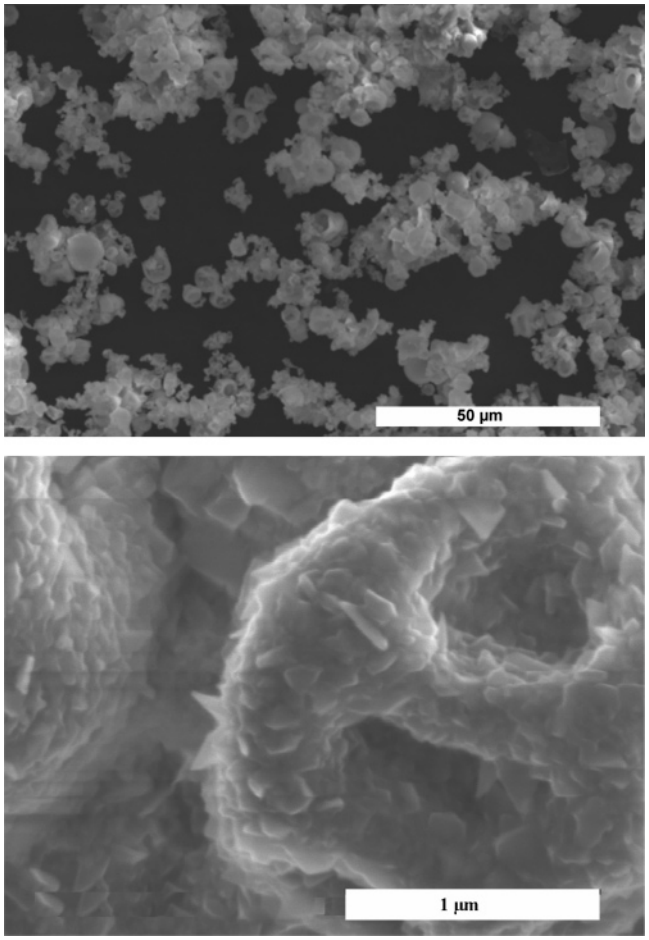

Figure 5. SEM micrographs of Li_2ZrO_3-SD calcined at 873 K: (A) low magnification, (B) high magnification.

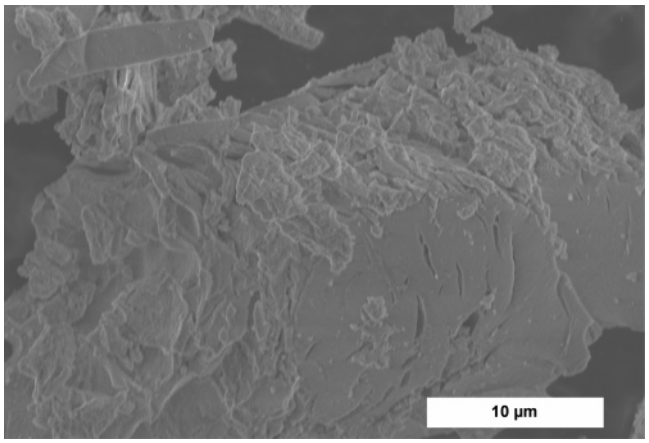

Figure 6. SEM micrograph of Li_2ZrO_3-D calcined at 873 K.

with holes resembling a doughnutlike shape were found. This particular morphology originates from the drying/calcination of the spherical droplets produced during spray drying. The droplets collapse to doughnutlike objects. As presented above, when the dried powders are heated to a certain temperature, the oxidation of the organic compounds leads to a smoldering process involving gas evolution. This significant gas evolution results in agglomerated particles with mesopores and macropores. As observed in Figure 6, Li_2ZrO_3-D presents a more irregular and packed structure with larger particle sizes.

Table 1. Nitrogen Sorption and Mercury Porosimetry Properties of the Prepared Samples Calcined at 873 K

sample	BET surface area (m^2/g)	pore volume[a] (cm^3/g)	pore volume[b] (cm^3/g)
Li_2ZrO_3-SD	5	0.017	0.51
Li_2ZrO_3-D	4	0.008	0.60

[a] N_2 sorption. [b] Hg porosimetry.

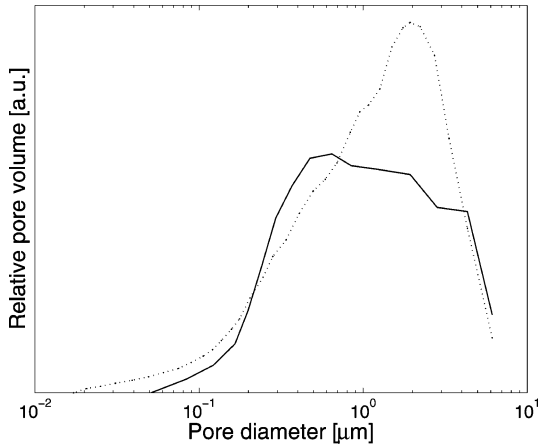

Figure 7. Pore size distribution of the prepared samples calcined at 873 K: (-) Li_2ZrO_3-SD, (−) Li_2ZrO_3-D.

3.1.3. Surface Area and Pore Characteristics. Table 1 shows BET surface areas and the pore size characteristics of the prepared samples, calculated by nitrogen sorption and mercury porosimetry. The reported BET surface areas for Li_2ZrO_3-SD and Li_2ZrO_3-D are 5 and 4 m^2/g, respectively. It seems that the use of spray drying does not lead to a significant increase in the surface area of the prepared samples. However, both Li_2ZrO_3-SD and Li_2ZrO_3-D show a surface area higher than what is reported for Li_2ZrO_3 prepared by solid-state reaction (<1 m^2/g).[24]

The pore volume was measured by two techniques: nitrogen sorption, accounting for the porosity due to micropores and mesopores, and mercury porosimetry, for the determination of both mesopores and macropores. In both samples, two regimes of pores were observed: mesopores and macropores. The sample prepared by spray drying showed a larger volume of mesopores according to N_2 physisorption measurements. However, this volume is almost negligible compared to the total pore volume measured by Hg porosimetry. Figure 7 shows the pore size distribution measured by Hg porosimetry for the two samples. A total pore volume between 0.5 and 0.6 cm^3/g was measured for the two samples. The spray dried Li_2ZrO_3 shows a broader pore size distribution.

3.2. Thermodynamic Properties. Figure 8 shows the equilibrium partial pressure of CO_2 during the carbonation reaction of Li_2ZrO_3 in the temperature interval from 350 to 1000 K. The equilibrium temperature of Li_2ZrO_3 was calculated to be 973 K when $P_{CO_2} = 1$. Accordingly, a further increase in the reaction temperature will result in the reverse reaction of eq 1, independently of the reaction atmosphere. Thus, the CO_2 capture is thermodynamically favored at lower temperatures. For instance, the partial pressure of CO_2 in the equilibrium at 842 and 610 K is 3.6×10^{-3} and 1.2×10^{-3} bar, respectively. Therefore, Li_2ZrO_3 can take CO_2 in a wide temperature range: from ambient to 973 K. However,

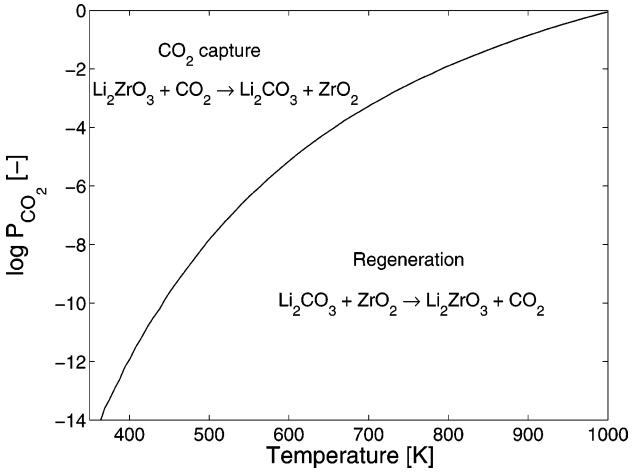

Figure 8. Equilibrium partial pressure of carbon dioxide at different temperatures. Total pressure: 1 bar.

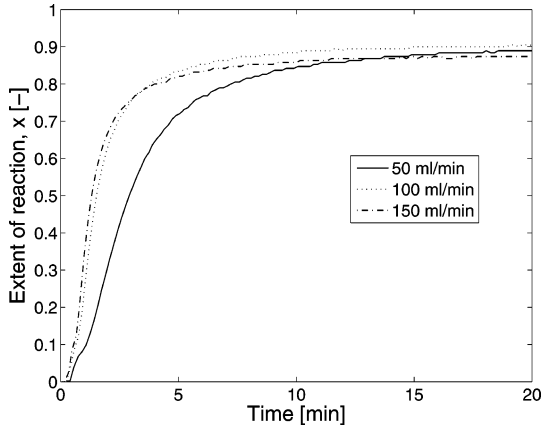

Figure 9. CO_2 uptake rates over Li_2ZrO_3-SD under different flow rates at 848 K.

capture rates at low temperatures are presumably slow because of kinetic limitations.[26,28]

3.3. CO_2 Capture/Regeneration Properties. *3.3.1. CO_2 Capture Properties.*

Figure 9 shows the uptake curves on Li_2ZrO_3-SD at different CO_2 flow rates. The operation temperature is 848 K. The capture rate increases considerably with the flow rate from 50 to 100 mL/min. No further significant increase in the capture rate is observed with increasing flow rates. Therefore, the CO_2 uptake curves were always measured at a minimum total flow of 100 mL/min to ensure no mass transfer limitations, which is essential for kinetic studies. In this matter, the TEOM is a powerful tool for the study of capture/regeneration kinetics compared with the conventionally used thermogravimetric microbalance (TGA). During TGA operation, the reactive mixture passes a basket containing the sample, resulting in important buoyancy and flow concerns. The bypass fraction is usually larger than 0.7, and bed diffusion may be the dominant transport mode through the sample located in the basket.[49] Instead, the TEOM combines the advantages of the conventional microbalance and the fixed bed reactor, allowing kinetic studies with high resolution and short response time under real operation conditions.

The relative mass increase from the capture of CO_2 for both Li_2ZrO_3-SD and Li_2ZrO_3-D at 848 K under a stream of

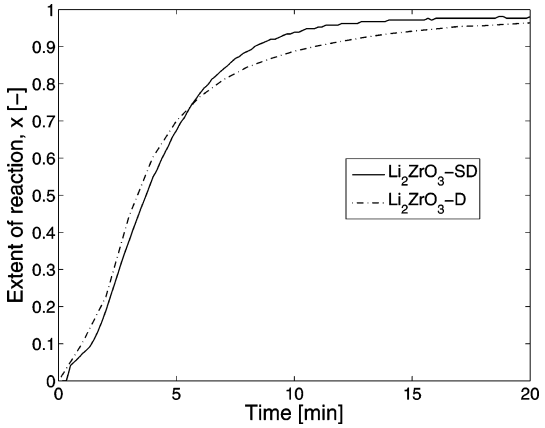

Figure 10. Comparison of the CO_2 capture properties of Li_2ZrO_3-SD and Li_2ZrO_3-D at 848 K and $P_{CO_2} = 1$ bar.

100 mL/min of CO_2 is presented in Figure 10. According to the plot, no large differences in capture properties of the two samples are observed at 848 K. Saturation of the acceptor is reached in both cases within 10 min. The same trend has been found for the rest of the tested temperatures, where the observed differences are so small that they are considered to be within the experimental error. As a result, the effect of the two different drying procedures followed in this study does not seem to be very important. This was expected, because similar BET surface areas and total pore volumes were measured for both samples, although the SEM images are very different. Therefore, the rest of the discussion will be based on Li_2ZrO_3-SD, assuming that similar results can be applied to Li_2ZrO_3-D.

The uptake curves shown in Figure 10 represent a breakthrough in the carbon dioxide capture rate for Li_2ZrO_3 compared to its counterparts prepared by solid-state reaction. Li_2ZrO_3 was reported for the first time as a good candidate for the CO_2 removal at high temperatures by Nakagawa et al. in 1998.[33] Nakagawa et al.[33] claimed that Li_2ZrO_3 powder can react immediately with CO_2 in the range 723−823 K. Moreover, the products can react and return reversibly to Li_2ZrO_3 at temperatures above 923 K. Several studies have been carried out afterward on the synthesis and properties of both pure and promoted Li_2ZrO_3.[24−29,31,35,37−39]

Ida *et al.* carried out a study about the capture properties of pure and modified Li_2ZrO_3 prepared by solid-state reactions. According to their investigation, pure Li_2ZrO_3 needed more than 50 h to reach saturation at 873 K.[25] Modification of Li_2ZrO_3 with Li_2CO_3/K_2CO_3 carbonate on lithium zirconate improved CO_2 capture rates considerably; modified Li_2ZrO_3 could reach saturation within 200 min at 873 K. Ohashi et al. have done a similar study.[29] They also concluded that the capture rate of pure Li_2ZrO_3 was slow in the studied range of temperatures. However, the uptake was accelerated by the K_2CO_3 additive, in this case reaching saturation within 150 min at 773 K. Slightly faster kinetics was reported by Xiong et al. also for a potassium-doped sample.[24] The acceptor was saturated after 60 min on stream at temperatures from 773 to 923 K. Doping K_2CO_3 into Li_2ZrO_3 increases the rate because of the formation of a eutectic molten carbonate composed of Li_2CO_3 and K_2CO_3 at high temperatures. Although the melting points of Li_2CO_3 and

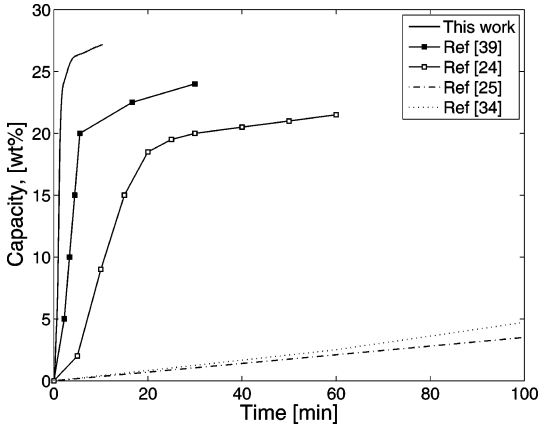

Figure 11. Comparison of the CO_2 capture properties of Li_2ZrO_3 prepared by the soft-chemistry route (2.2:1 Li:Zr) with other reported samples. $P_{CO_2} = 1$ bar. $T = 848$ K (this work), 773 K (refs 24 and 39), 873 K (refs 25 and 34).

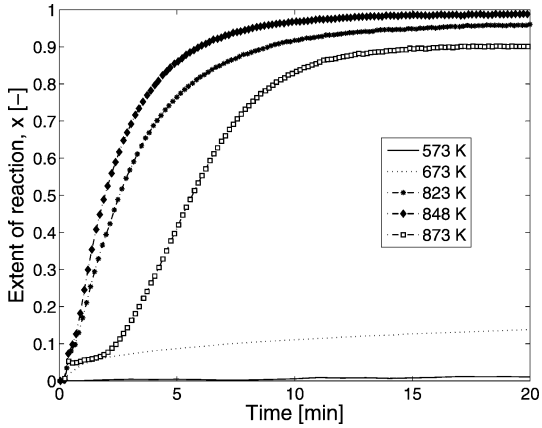

Figure 12. Extent of reaction, x, of the CO_2 capture on Li_2ZrO_3-SD when $P_{CO_2} = 1$ at different temperatures.

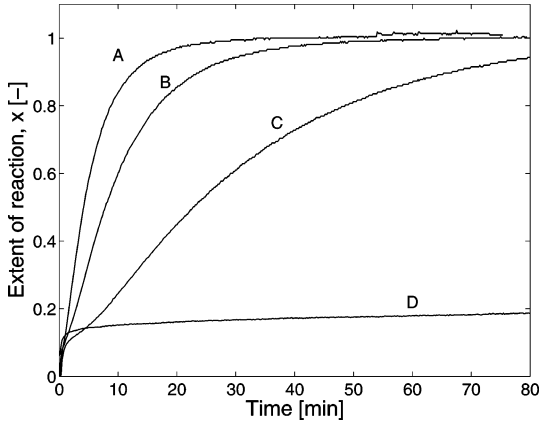

Figure 13. Extent of reaction, x, of the CO_2 capture on Li_2ZrO_3-SD at 823 K and P_{CO_2} equal to (A) 0.7, (B) 0.5, (C) 0.3, and (D) 0.1.

K_2CO_3 are 996 and 1164 K, respectively, the melting point of their mixture is much lower with a minimum at 771 K.[31] This molten carbonate can significantly enhance CO_2 diffusion compared to the solid shell in the case of pure Li_2ZrO_3. Fauth et al. have also studied the CO_2 uptake on pure Li_2ZrO_3 powder.[37] They also found a very slow uptake with time on stream. The performance of the powder was greatly improved by the doping with binary alkali carbonate, binary alkali/alkaline earth carbonate, and ternary alkali carbonates. The formation of a eutectic molten carbonate layer on the outer surface of the Li_2ZrO_3 powders was also identified as the reason for the faster uptake, facilitating the transfer of CO_2 during the removal process.[37] Nevertheless, the capture rate of the pure Li_2ZrO_3 prepared in the present work[38] is several times faster than the capture rate of any of the reported pure/modified Li_2ZrO_3 prepared by solid-state reaction.[24,25,29,31,37] A direct comparison of the experimental data obtained in this work with data previously reported can be found in Figure 11. As described above, pure Li_2ZrO_3 prepared in this work is much faster than pure[25,34] and K-doped[24] Li_2ZrO_3 prepared by solid-state reaction. Similar observations have also recently been reported by Yi et al.[39] It should be noticed that the testing conditions in the compared samples are slightly different from the conditions in this study. 873 K was used as reaction temperature in refs 25 and 34, whereas 773 K was used in refs 24 and 39, although $P_{CO_2} = 1$ bar was used in all cases.

The effect of the working temperature and the partial pressure of carbon dioxide have also been studied. Both parameters strongly affect the uptake rate. Figure 12 shows the uptake curves for Li_2ZrO_3-SD at five different temperatures (573, 673, 823, 848, and 873 K). According to the thermodynamics presented in Figure 8, Li_2ZrO_3 is able to take CO_2 in a large range of temperatures, from room temperature to 973 K. However, the capture rate is slow at low temperatures (<673 K). The rate increases considerably when the working temperatures are higher than 673 K and, according to Figure 12, especially when the temperature is 848 K, going from about 3 mg of CO_2 g^{-1} min^{-1} at 673 K to about 83 mg of CO_2 g^{-1} min^{-1} at 873 K. Increasing the temperature from 848 to 873 K leads to a decrease in the uptake rate from about 83 to about 34 mg of CO_2 g^{-1} min^{-1}. This phenomenon is due to the importance of the reverse reaction (regeneration) that is enhanced at higher temperatures. The equilibrium partial pressure of CO_2 will increase with temperature. Xiong et al.[24] also studied the influence of the temperature on the CO_2 capture on modified lithium Li_2ZrO_3. They also reported that the temperature effect on the uptake rates depends on both thermodynamic and kinetic factors. According to their study, the maximum rates were also obtained at 848 K. Thus, an optimum working temperature of 848 K is recommended on the basis of the results in Figure 12.

The capture rate is also strongly dependent on the partial pressure of carbon dioxide in the feed stream. Figure 13 shows the CO_2 uptake profiles of Li_2ZrO_3-SD at 823 K when P_{CO_2} goes from 0.1 to 0.7 atm. As expected, the capture rate decreases with decreasing the relative CO_2 amount, becoming considerably lower at partial pressures of CO_2 below 0.1 atm. The same trend has been found for other temperatures. The reaction rate is especially affected at low P_{CO_2} (<0.1 atm), because the CO_2 concentration becomes close to the equilibrium partial pressure of CO_2: 0.025 atm when the working temperature is 823 K.

3.3.2. Regeneration. Even though several efforts have been made in the literature to describe the CO_2 capture properties of Li_2ZrO_3, not much information is found about the regeneration of the material, which is actually the most

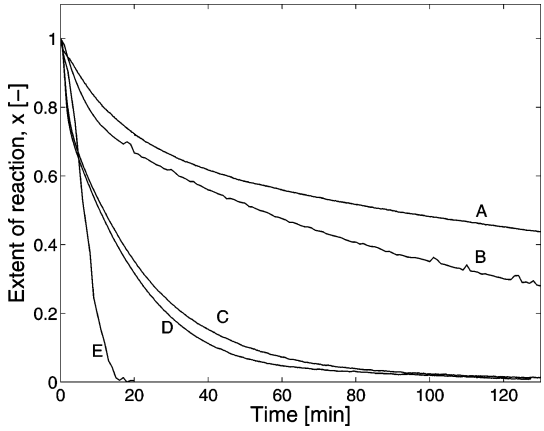

Figure 14. Extent of the regeneration under an Ar atmosphere at (A) 798, (B) 848, (C) 873, (D) 893, and (E) 923 K.

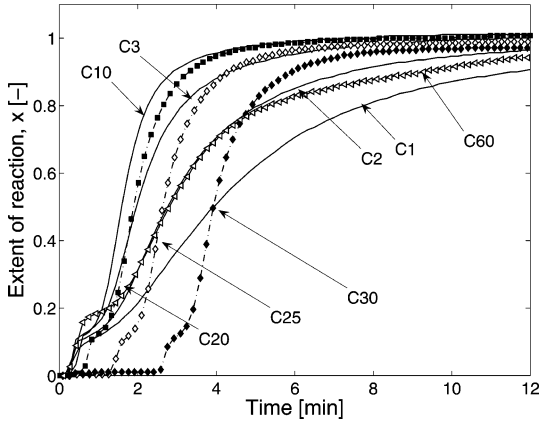

Figure 15. Extent of reaction, x, of the CO_2 capture on Li_2ZrO_3-SD at 848 K during successive cycles. Regeneration conditions: 923 K, 100 mL/min Ar.

energy demanding part of the process. In this investigation, the regeneration of Li_2ZrO_3 has been studied at different temperatures under an inert atmosphere. More specifically, in order to proceed with the regeneration of the acceptor, the temperature of the reactor is increased from the capture temperature, T_c, to the regeneration temperature, T_r, with a heating rate of 10 K/min (see Figure 1). As described earlier, the reaction atmosphere is changed from the reaction mixture to pure Ar at a constant flow rate of 100 mL/min.

Figure 14 shows the regeneration profiles of Li_2ZrO_3-SD at different regeneration temperatures, T_r, from 798 to 923 K. The regeneration time is strongly dependent on the regeneration temperature, going from several hours at 798 K to a few minutes when the temperature is increased to 923 K. Fauth et al. have recently reported the regeneration of both pure and modified Li_2ZrO_3 prepared by solid-state reactions[37] in which the temperature for the regeneration was chosen to be 1023 K under Ar atmosphere. At this high temperature, complete regeneration of the acceptor was reached after more than 60 min. Only small differences in the rate of CO_2 emission were observed for both pure and modified Li_2ZrO_3 samples.

Thus, pure nanocrystalline Li_2ZrO_3 prepared in this study represents not only a significant improvement in the CO_2 capture but also in the regeneration stage, allowing faster regeneration. It should be pointed out that the regeneration is carried out in Ar in the present work. Higher temperatures (~973 K) are necessary in the case in which the regeneration in CO_2 is preferred to obtain high concentrations of CO_2 for transport and storage. Regeneration in CO_2 has not been investigated because of the limitation in the operating temperature of the TEOM.

3.3.3. Stability of Performance. The stability of capture−regeneration performance of Li_2ZrO_3-SD has been tested over 100 cycles. The capture was carried out at 848 K under 100 mL/min of CO_2 and regeneration at 923 K in an Ar atmosphere. Figure 15 shows the CO_2 capture profiles during selected successive cycles. The capture rate is enhanced considerably during the first 10 cycles, whereas no losses in the capacity are recorded. More specifically, the reaction rate increased from about 68 mg of CO_2 g^{-1} min^{-1} at cycle 2 to about 200 mg of CO_2 g^{-1} min^{-1} after 10 cycles. With an increasing number of cycles, an activation period accompanied by a slight loss in the capacity is observed. The CO_2 removal does not take place until this barrier, which can go from seconds to several minutes, is overcome. However, this is a reversible phenomenon that disappeared completely after 60 cycles. This observation is reproducible. The reason for the appearance/disappearance of this barrier during the capture/regeneration reactions is not yet clear. A tentative explanation is that capture and regeneration cycles are changing the structure of the nanoparticles, resulting in significant changes in rates of the nucleation of Li_2CO_3 and ZrO_2 during cycles. However, a further detailed study is necessary to gain a precise understanding of the induction behavior. On the other hand, the total capacity of the acceptor at the end of the study (100 capture/regeneration cycles) was maintained above 90% of the capacity of the fresh sample.

3.3.4. Mechanism. The reaction between Li_2ZrO_3 and CO_2 to form Li_2CO_3 and ZrO_2 can be understood as a recrystallization process. The first step in crystallization is to form a primary nucleation. In this case, a large supersaturation driving force is necessary to initiate the nucleation. Accordingly, a threshold concentration of CO_2 may be necessary for starting the carbonation reaction. As shown in Figure 13, the CO_2 capture is limited at P_{CO_2} below 0.1 bar. To clarify possible limitations of nucleation at low partial pressure of CO_2, we designed an experiment in which the capture was initiated with a feed of 50% CO_2; after a few minutes, the feed was changed to 10% CO_2. At this point, the measured uptake of CO_2 was stopped. This indicates that the limitation on the capture at low partial pressures of CO_2 is more an effect of thermodynamic and/or diffusion limitations than of the nucleation in the crystallization process.

The existence of a complicated mechanism of CO_2 capture of Li_2ZrO_3 was discussed above. An in situ HTXRD investigation has been carried out to gain some knowledge about the reaction mechanism. Figure 16 shows a typical result from a CO_2 capture experiment. All diffractograms were measured at 848 K and a P_{CO_2} between 0.5 and 0.7 bar. There is a delay of 15 min between the start of scan and the start of the next one. From the figure, it can be seen that the intensity of the Li_2ZrO_3 diffraction lines decreases

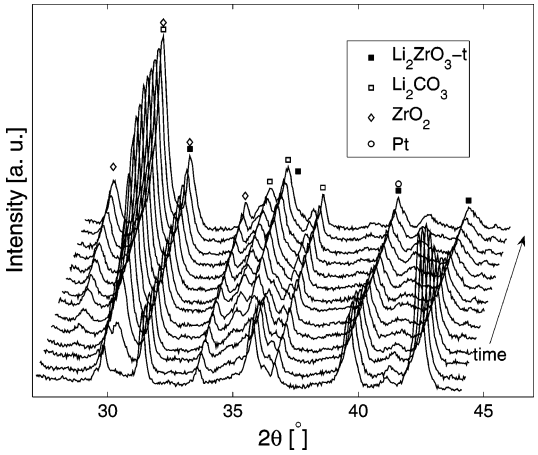

Figure 16. In situ HTXRD study of the removal of CO_2 by Li_2ZrO_3-SD at 848 K. (■ = Li_2ZrO_3, □ = Li_2CO_3, ◇ = ZrO_2, ○ = Pt)

progressively in favor of the formation of both Li_2CO_3 and ZrO_2 according to eq 1. The reverse reaction is carried out during regeneration. The Pt diffraction line stems from the sample holder. Two capture−regeneration cycles were carried out, and no indication of any intermediate compound could be identified. The only difference in the successive cycles was related to the intensity of the ZrO_2 reflections that were more pronounced after some cycles.

Another purpose of the in situ XRD study of CO_2 capture and regeneration was to study the mechanism of the induction behavior. However, very limited information can be obtained in this respect because of the low time resolution of XRD compared to the time scale in the CO_2 capture.

4 Conclusions

Nanocrystalline Li_2ZrO_3 has been prepared by a soft-chemistry route using lithium acetate and zirconyl nitrate as precursors. The nanocrystalline nature of the material is a result of the mild conditions used during the synthesis. Specifically, the calcination temperature was found to be a critical parameter for controlling the crystalline structure. The optimum calcination temperature was set to 873 K, and tetragonal nanocrystalline Li_2ZrO_3 was obtained. Special attention has been given to the study of the CO_2 capture and regeneration properties of the material. The tetragonal and nanocrystalline nature of the resulting Li_2ZrO_3 give rise to improved capture of CO_2 in a wide temperature range. An operational window for CO_2 capture was found at temperatures between 773 and 873 K, whereas a maximum rate for CO_2 capture was obtained at 848 K. In addition, the kinetics of the regeneration have been considerably improved, allowing a fast regeneration at relatively low temperatures. Furthermore, TEOM has been shown to be a powerful technique for CO_2 kinetic measurements.

The appearance and disappearance of an induction period during the CO_2 capture on Li_2ZrO_3 is observed. However, further studies are necessary to clarify this phenomenon as well as the low capture rates at low CO_2 partial pressures.

Acknowledgment. The financial support from the Research Council of Norway is greatly acknowledged.

CM061515D